LA-3992

LOS ALAMOS SCIENTIFIC LABORATORY
of the
University of California
LOS ALAMOS • NEW MEXICO

An Application of the Lagrangian Functional to Collapsing Reactor Cross Sections

UNITED STATES
ATOMIC ENERGY COMMISSION
CONTRACT W-7405-ENG. 36

This report expresses the opinions of the author or authors and does not necessarily reflect the opinions or views of the Los Alamos Scientific Laboratory.

Printed in the United States of America. Available from Clearinghouse for Federal Scientific and Technical Information National Bureau of Standards, U. S. Department of Commerce Springfield, Virginia 22151

Price: Printed Copy $3.00; Microfiche $0.65

LA-3992
UC-80, REACTOR
TECHNOLOGY
TID-4500

LOS ALAMOS SCIENTIFIC LABORATORY
of the
University of California
LOS ALAMOS • NEW MEXICO

Report written: September 1967
Report distributed: December 31, 1968

An Application of the Lagrangian Functional to Collapsing Reactor Cross Sections

by

Jeffrey S. Philbin
Byron M. Carmichael

AN APPLICATION OF THE LAGRANGIAN FUNCTIONAL TO COLLAPSING REACTOR CROSS SECTIONS

by

Jeffrey S. Philbin and Byron M. Carmichael

ABSTRACT

The characteristic Lagrangian functional for the infinite-medium transport equation has been used to derive a complete set of collapsing formulas for broad-group cross sections. These formulas include adjoint-flux weighting but reduce to regular-flux weighting formulas when the adjoint spectrum is constant. The collapsed cross sections were used to generate broad-group regular and adjoint fluxes, which agreed very well with the values predicted by the initial fine-group spectra. This formulation also ensures the preservation of the eigenvalue.

1. INTRODUCTION

The continuous energy spectrum of the neutrons in a nuclear reactor ranges from thermal energies to about 10 MeV. Equations formulated to describe the neutron density in a reactor, such as the Boltzmann transport equation, therefore, include energy-dependent cross sections in the neutron balances. The energy-dependent cross sections are simply probabilities that a specific neutron reaction will occur.

The traditional approach to solving such integro-differential reactor equations has been to formulate a number of discrete energy groups, the neutron cross sections being assumed constant within each group. In the case of an infinite, isotropic medium, this leads to a set of linearly independent multigroup equations which can be solved simultaneously.

Accurate solutions can be ensured by using a sufficiently fine group structure. However, fine-group reactor analysis calculations, especially those for finite-geometry problems, take a considerable amount of time even on high-speed digital computers. It is, therefore, desirable to reduce the number of groups and still retain an accurate model for reactor computations. In this paper, a variational analysis of the multigroup system is presented. This analysis leads to a set of collapsing formulas for cross sections which include adjoint-flux weighting. This collapsing method preserves the eigenvalue of the reactor and the flux distributions predicted by the fine-group calculations.

2. THEORY

Given any system described by linear operator equations, an adjoint solution can be defined together with a Lagrangian functional whose stationary property is equivalent to the equations of the system.[1] A Lagrangian functional can, therefore, be formulated for the transport equation. For simplicity, an infinite medium and isotropic scattering are assumed. The steady-state transport equation for such a system is

$$\mu^t(E)\,\phi(E) = \int_0^\infty dE'\,\mu^s(E'\to E)\,\phi(E') + \frac{\chi(E)}{k}\int_0^\infty dE'\,\nu(E')\,\mu_f(E')\,\phi(E'), \tag{1}$$

or, in multigroup form,

$$\mu_g^t\,\phi_g = \sum_{g'=1}^{NFGPS} \phi_{g'}\left[\mu^s(g'\to g) + \frac{\chi_g}{k}\langle\nu\mu_f\rangle_{g'}\right]. \tag{2}$$

The adjoint equation is

$$\mu^t(E)\ \phi^*(E) = \int_0^\infty dE'\ \mu^s(E\to E')\ \phi^*(E') + \frac{\nu(E)\ \mu_f(E)}{k} \int_0^\infty dE'\ \chi(E')\ \phi^*(E'), \tag{3}$$

or, in multigroup form,

$$\mu_g^t\ \phi_g^* = \sum_{g'=1}^{NFGPS} \phi_{g'}^* \left[\mu^s(g\to g') + \frac{\langle \nu\mu_f\rangle_g}{k}\ \chi_{g'}\right], \tag{4}$$

where

$\mu^i \equiv$ macroscopic cross section for i reaction

$k \equiv$ eigenvalue of the reactor

$\chi \equiv$ fission spectrum

$\phi \equiv$ regular flux

$\phi^* \equiv$ adjoint flux

NFGPS $\equiv$ number of fine groups.

In operator form, these equations are

$$H\phi(E') = f(E) \equiv 0 \tag{5}$$

and

$$H^*\phi^*(E') = g^*(E) \equiv 0 \tag{6}$$

where the operators H and H* are

$$H = \int_0^\infty dE' \left[-\mu^t(E')\ \delta(E - E') + \mu^s(E'\to E) + \frac{\chi(E)}{k}\ \nu(E')\ \mu_f(E')\right] \tag{7}$$

and

$$H^* = \int_0^\infty dE' \left[-\mu^t(E)\ \delta(E' - E) + \mu^s(E\to E') + \frac{\chi(E')}{k}\ \nu(E)\ \mu_f(E)\right]. \tag{8}$$

The Lagrangian functional for this system is

$$F = -(\phi^*, H\phi) \equiv -\int_0^\infty dE\ \phi^*(E)\ H\phi(E'). \tag{9}$$

This functional has stationary properties with respect to ϕ^* and ϕ which are equivalent to Eqs. 1 and 3 (i.e., perturbing F through $\phi^* \to \phi^* + \delta\phi^*$ yields $F + \delta F$ and setting $\delta F = 0$ gives back Eq. 1; perturbing F through $\phi \to \phi + \delta\phi$ gives back Eq. 3).

In multigroup form, the functional becomes

$$F = \sum_g^{NFGPS} \phi_g^*\ \mu_g^t\ \phi_g - \sum_g^{NFGPS} \phi_g^* \sum_{g'}^{NFGPS} \phi_{g'}\ \mu_{g'g}^s - \sum_g^{NFGPS} \phi_g^* \sum_{g'}^{NFGPS} \frac{\chi_g}{k} \langle \nu\mu_f\rangle_{g'}\ \phi_{g'}\ , \tag{10}$$

where $\mu_{g'g}^s = \mu^s(g'\to g)$ is the transfer scattering cross section from group g' to group g, and the stationary properties of the functional are retained.

We now assume that a set of broad-group cross sections can be found such that the reactor has the same eigenvalue as in the previous fine-group formulation.

The Lagrangian functional in terms of the new parameters can be written down at once:

$$F = \sum_G^{NBGPS} \phi_G^*\ \mu_G^t\ \phi_G - \sum_G^{NBGPS} \phi_G^* \sum_{G'}^{NBGPS} \phi_{G'}\ \mu_{G'G}^s - \sum_G^{NBGPS} \phi_G^* \sum_{G'}^{NBGPS} \frac{\chi_G}{k} \langle \nu\mu_f\rangle_{G'}\ \phi_{G'}. \tag{11}$$

As before, the stationary properties of F are retained. The eigenvalue of the reactor is assumed to be the same in both functionals.

The Lagrangian functionals from the fine- and broad-group formulations must be equal if they describe the same system. We ensure this equality by equating corresponding terms from each of the functionals. This operation leads to a natural and necessary definition of the broad-group cross sections in terms of the fine-group cross sections, regular fluxes, and adjoint fluxes. For example,

$$\sum_g^{NFGPS} \phi_g^*\ \mu_g^t\ \phi_g = \sum_G^{NBGPS} \phi_G^*\ \mu_G^t\ \phi_G. \tag{12}$$

Since the broad-group parameters are still undefined, the individual broad-group terms may be defined as follows:

$$\phi_G^*\ \mu_G^t\ \phi_G = \sum_{g\in G} \phi_g^*\ \mu_g^t\ \phi_g. \tag{13}$$

This leads to the collapsing formula for μ_G^t

$$\mu_G^t = \frac{\sum_{g\epsilon G} \phi_g^* \mu_g^t \phi_g}{\phi_G^* \phi_G}, \tag{14}$$

where μ_g^t are known, and ϕ_g, ϕ_g^* are the solutions of Eqs. 2 and 4. From the fine-group spectra, ϕ_G is obtained by

$$\phi_G = \sum_{g\epsilon G} \phi_g. \tag{15}$$

The expression for ϕ_G^* in terms of the fine-group spectra is derived by combining Eq. 15 with Eq. 14 for the special case when μ_g^t is constant, which yields

$$\phi_G^* = \frac{\sum_{g\epsilon G} \phi_g^* \phi_g}{\sum_{g\epsilon G} \phi_g}. \tag{16}$$

These values for ϕ_G and ϕ_G^*, in addition to being used in the collapsing formulas (see Eq. 14), will also serve as standards to which we can compare the broad-group spectra obtained by solving Eqs. 2 and 4 with collapsed cross-section sets. The cross sections of the new collapsing method, as well as the regular-flux-weighted cross sections, will be used for this comparison.

This procedure of obtaining the broad-group fluxes directly from the fine-group spectra eliminates the need for computing ϕ_G and ϕ_G^* with regular-flux-weighted cross sections as suggested by Little and Hardie.[2]

The collapsed cross sections derived from the Lagrangian functional (LF-weighted cross sections) can now be written entirely in terms of fine-group spectra and cross sections.

The LF collapsing formulas are

$$\mu_G^t = \frac{\sum_{g\epsilon G} \phi_g^* \mu_g^t \phi_g}{\sum_{g\epsilon G} \phi_g^* \phi_g}, \tag{17}$$

$$\mu_{G'G}^s = \frac{\sum_{g\epsilon G} \sum_{g'\epsilon G'} \phi_{g'} \mu_{g'g}^s \phi_g^*}{\sum_{g'\epsilon G'} \phi_{g'} \left(\sum_{g\epsilon G} \phi_g^* \phi_g \Big/ \sum_{g\epsilon G} \phi_g \right)}, \tag{18}$$

$$\langle \nu\mu_f \rangle_{G'} = \frac{\sum_{g'\epsilon G'} \phi_{g'} \langle \nu\mu_f \rangle_{g'}}{\sum_{g'\epsilon G'} \phi_{g'}}, \tag{19}$$

and

$$\chi_G = \frac{\sum_{g\epsilon G} \chi_g \phi_g^*}{\sum_{g\epsilon G} \phi_g^* \phi_g \Big/ \sum_{g\epsilon G} \phi_g}. \tag{20}$$

The rest of the broad-group cross sections are easily derived from the above results:

$$\mu_G^f = \frac{\nu\mu_{f\,G}}{\nu_G}, \tag{21}$$

$$\mu_G^s = \sum_{G'=1}^{NBGPS} \mu_{GG'}^s, \tag{22}$$

$$\mu_G^a = \mu_G^t - \mu_G^s, \tag{23}$$

and

$$\mu_G^c = \mu_G^a - \mu_G^f. \tag{24}$$

These formulas can be applied to the microscopic cross sections as well. This collapsing scheme preserves the multiplication factor of the reactor. In all instances, the LF collapsing formulas reduce to the regular-flux-weighting formulas when the adjoint flux is a constant.

The same procedure applied to the time-dependent problem leads to a collapsing formula for the group velocities. Only one additional assumption is made:

$$\phi(E,t) = \phi_g e^{\alpha t}, \tag{25}$$

where $E_{g-1} < E < E_g$, and $\alpha \equiv$ stable inverse period.

The resulting multigroup equations and Lagrangian functional will then be the same as before, except that a time-absorption term appears along

with the total cross sections. The functional for the time-dependent multigroup problem is

$$F = \sum_{g'=1}^{NFGPS} \sum_{g=1}^{NFGPS} \phi_g^* \phi_g \left[\left(\mu_g^t + \frac{\alpha}{v_g} \right) \delta_{g'g} - \mu_{g'g}^s - \frac{\chi_g}{k} \langle \nu\mu_f \rangle_{g'} \right] . \quad (26)$$

Thus, the group velocities are collapsed as follows:

$$v_G = \frac{\sum_{g \in G} \phi_g^* \phi_g}{\sum_{g \in G} \frac{\phi_g^* \phi_g}{v_g}} . \quad (27)$$

The multigroup expression for the neutron lifetime in the infinite medium is derived from perturbation theory. If the lifetime is invariant under the transformation from fine groups to broad groups,

$$\ell = \frac{\sum_{g=1}^{NFGPS} \frac{\phi_g^* \phi_g}{v_g}}{k} = \frac{\sum_{G=1}^{NBGPS} \frac{\phi_G^* \phi_G}{v_G}}{k} . \quad (28)$$

This approach is entirely consistent with the Lagrangian functional formulation and lends further support to the correctness of this collapsing procedure.

3. REGULAR-FLUX-WEIGHTING FORMULAS

Sets of cross sections are usually collapsed by regular-flux weighting techniques. The regular-flux-collapsing formulas are

$$\mu_G^t = \frac{\sum_{g \in G} \phi_g \mu_g^t}{\sum_{g \in G} \phi_g} , \quad (29)$$

$$\langle \nu\mu_f \rangle_G = \frac{\sum_{g \in G} \phi_g \langle \nu\mu_f \rangle_g}{\sum_{g \in G} \phi_g} , \quad (30)$$

$$\mu_{G'G}^s = \frac{\sum_{g \in G} \sum_{g' \in G'} \phi_{g'} \mu_{g'g}^s}{\sum_{g' \in G} \phi_g} , \quad (31)$$

$$\chi_G = \sum_{g \in G} \chi_g , \quad (32)$$

and

$$v_G = \frac{\sum_{g \in G} \phi_g}{\sum_{g \in G} \frac{\phi_g}{v_g}} . \quad (33)$$

As pointed out before (see Eqs. 21-24), the rest of the broad-group cross sections may easily be derived from the above results. Equations 29, 30, and 31 are developed by equating the reaction rates of the broad and fine groups, where the broad-group flux is given by

$$\phi_G = \sum_{g \in G} \phi_g . \quad (34)$$

4. SOLUTION OF THE INFINITE-MEDIUM MULTIGROUP EQUATIONS

As demonstrated in Sections 2 and 3, one can obtain reduced sets of cross sections in terms of the fine-group parameters.

For the special case of an infinite medium, the regular fluxes and adjoint fluxes are obtained by solving Eqs. 2 and 4.

We begin the solution by imposing normalization conditions,

$$\sum_{g=1}^{NFGPS} \frac{\phi_g}{k} \langle \nu\mu_f \rangle_g = \sum_{g=1}^{} \frac{\phi_g^*}{k} \chi_g = 1, \quad (35)$$

on Eqs. 2 and 4. These conditions provide us with a definition for k and transform Eqs. 2 and 4 into two inhomogeneous systems of equations:

$$\mu_g^t \phi_g - \sum_{g'=1}^{NFGPS} \phi_{g'} \mu_{g'g}^s = \chi_g \quad (36)$$

$$\mu_g^t \phi_g^* - \sum_{g'=1}^{NFGPS} \phi_{g'}^* \mu_{gg'}^s = \langle \nu\mu_f \rangle_g . \quad (37)$$

Equation 36 represents a set of linearly independent equations for the unknowns ϕ_g. Similarly, Eq. 37 is a set of linearly independent equations for the unknowns ϕ^*_g. These two inhomogeneous systems can be written in matrix form and solved separately. With tensor notation and the summation convention for repeated indices, Eqs. 36 and 37 become

$$\left[\mu^t_g \delta_{g',g} - \mu^s_{g',g}\right]\phi_{g'} = \chi_g \tag{38}$$

$$\left[\mu^t_g \delta_{g',g} - \mu^s_{gg'}\right]\phi^*_{g'} = \nu\mu_{f\,g} \,. \tag{39}$$

In this form, the individual matrix elements are easily identified. Let us now define

$\delta_{gg'} \equiv$ Kronecker delta,

$\underline{\phi} \equiv$ column vector of regular fluxes, ϕ_g,

$\underline{\phi^*} \equiv$ column vector of adjoint fluxes, ϕ^*_g,

$\underline{\underline{B}} \equiv$ g x g square coefficient matrix of the adjoint-fluxes whose individual elements are:

$$B_{gg'} = \mu^t_g \delta_{gg'} - \mu^s_{gg'},$$

$\underline{\underline{B}}^t \equiv$ transpose of $\underline{\underline{B}}$ = coefficient matrix of the regular fluxes,

(Note: $B^t_{gg'} = B_{g'g} = \left[\mu^t_g \delta_{g'g} - \mu^s_{g'g}\right]$)

$\underline{\chi} \equiv$ inhomogeneous column vector of the regular flux system,

and

$\underline{\nu\mu_f} \equiv$ inhomogeneous column vector of the adjoint flux system.

The matrix systems to be solved are

$$[\underline{\underline{B}}^t][\underline{\phi}] = [\underline{\chi}] \tag{40}$$

$$[\underline{\underline{B}}][\underline{\phi^*}] = [\underline{\nu\mu_f}], \tag{41}$$

and the solutions to these systems are

$$\underline{\phi} = [\underline{\underline{B}}^t]^{-1}\,[\underline{\chi}] \tag{42}$$

$$\underline{\phi^*} = [\underline{\underline{B}}]^{-1}\,[\underline{\nu\mu_f}]. \tag{43}$$

These solutions were obtained by matrix inversion on a computer with the Linear System Solver subroutine.* This subroutine can solve systems with as many as 59 groups in less than 10 sec. This matrix inversion method eliminates the time-consuming iteration method of solution.

* This subroutine, LA-FD04, can be obtained by writing to C Division of the Los Alamos Scientific Laboratory.

5. APPLICATIONS

The LF and regular-flux collapsing schemes were applied to three sets of reactor core cross sections:

(1) a 59-group set of thermal cross sections,[3]

(2) a 25-group set of thermal and nonthermal cross sections for a thermal reactor,[4] and

(3) a 16-group set of fast reactor cross sections.[5]

Fine-group cross sections were collapsed into a broad group over a range where the adjoint flux was flat or relatively flat. The collapsed cross sections, the broad-group regular fluxes from Eq. 15, and the broad-group adjoint fluxes from Eq. 16 were computed. Then a new set of broad-group fluxes was computed by solving Eqs. 42 and 43 (written for a reduced number of groups), with the collapsed cross sections forming the matrix elements.

Comparing these values with the broad-group regular and adjoint fluxes calculated previously from Eqs. 15 and 16 provides a check on the accuracy of the collapsed cross sections.

After the collapsed cross sections and the broad-group regular and adjoint fluxes were obtained, the eigenvalue was recomputed and compared to the initial eigenvalue. Agreement was observed to four or more significant figures for both LF and regular-flux weighting. This agreement was expected, since it can be shown theoretically that the eigenvalue for the infinite medium is unaffected by these two collapsing methods. The individual cross sections depend, of course, on the choice of the weighting function.

The LF and regular-flux-weighting methods for collapsing cross sections have been incorporated into two codes, CHILE and TAOS. The operational characteristics of these codes are described in Appendices A and B.

6. RESULTS

6.1 59-Group Set of UHTREX Thermal Cross Sections

Microscopic cross sections and atom densities for the UHTREX reactor[3] at Los Alamos Scientific Laboratory were the input data for this problem. The nuclides in the core mixture and their atom densities are given in Table I. The only nuclide

TABLE I

UHTREX CORE COMPOSITION

Nuclide	Atom Density (atoms/barn-cm)	Description
Aluminum	7.36127×10^{-5}	Absorber
Boron	1.10252×10^{-5}	Absorber
Iron	4.05971×10^{-5}	Absorber
Uranium-235	1.06540×10^{-5}	Absorber
Thorium-232	1.51100×10^{-4}	Absorber
Carbon (393°K)	8.10805×10^{-2}	Scatterer

with a scattering transfer matrix in the assembly was carbon. A group scattering transfer matrix, $\sigma^s(g' \to g)$, was constructed for carbon from a point scattering matrix, $\sigma^s(E_{g'} \to E_g)$. Appropriate source terms were derived for the thermal energy groups by calculating the probability of neutrons above the thermal boundary (3.056 eV) scattering into each of the 59 thermal groups.[4] The sources, normalized to 1, are:

$$S_{59} = 0.852$$
$$S_{58} = 0.148$$
$$S_g = 0.0 \qquad 0 \leq g \leq 57,$$

where 59 is the highest thermal energy group.

A code, THMOD, was designed to collapse this 59-group set of thermal cross sections by LF weighting. It is modeled after THERM1,[6] which executes the collapse by regular-flux weighting. THMOD can collapse both macroscopic and microscopic cross sections of a medium. The input specifications for THMOD are given in Appendix C.

The 59 groups were collapsed to 13 groups. The THMOD cross sections were compared with the THERM1 cross sections. Agreement was observed to four significant figures for macroscopic cross sections and, in general, to five significant figures for microscopic cross sections. These two different collapsing methods give similar results because the adjoint flux for this problem was nearly constant over the entire 59 groups. This close agreement was expected since $\langle \nu\mu_f \rangle_g / \mu_g^a$, the probability of a fission reaction in group g, is nearly constant in the thermal range. For such a case, the adjoint flux is nearly constant and the LF collapsing formulas reduce to the regular-flux collapsing formulas.

The LF cross sections were used in the multigroup equations to generate new regular and adjoint fluxes, and the agreement between these calculated fluxes and the broad-group fluxes defined in Eqs. 15 and 16 was remarkably good. The values agreed to four significant figures or better for all groups. The eigenvalue was accurately preserved after the collapse:

$k_\infty = 1.631$	59 groups
$k_\infty = 1.631$	13 groups (LF weighted)
$\delta k/k = 0.00$	59→13 groups.

Similar results were obtained with the regular-flux-weighted cross sections.

6.2 25-Group Set of UHTREX Cross Sections

This 25-group set[5] of cross sections is a combination of the 13 collapsed thermal cross sections just discussed and 12 nonthermal groups. The complete set is obtained as punched output from THERM1, with a table length of 13 for each group. CHILE requires a special set of reading cards to accommodate this set. The nuclides and atom densities are those given in Table II, but the nuclides are no longer classified as absorbers and scatterers, because an abbreviated transfer matrix has been defined for each nuclide in the mixture. Three collapsing routines were investigated: 25→6, 25→2, and 25→1. The 25-group regular and adjoint fluxes are shown in Figs. 1 and 2. Superimposed on the fine-group fluxes is a collapsed set of fluxes (the 6-group set). The adjoint flux for this thermal reactor is nearly constant. Thus, the difference between the LF-weighted and regular-flux-weighted cross sections will be less significant for UHTREX than for the Argonne fast reactor, which has an irregular (nonconstant) adjoint flux spectrum. Table II presents a 25-group set of microscopic cross sections for boron and sets collapsed to 6 and 2 groups by both LF and regular-flux weighting. The differences between the LF cross sections and the regular-flux-weighted cross sections become important if three-place accuracy is required for subsequent calculations. The agreement between the aluminum cross-section sets was slightly better than that for boron. The total macroscopic cross sections of the reactor (after collapsing by both methods) agreed to four significant figures for the 6-group sets and to three significant figures for the 2-group sets.

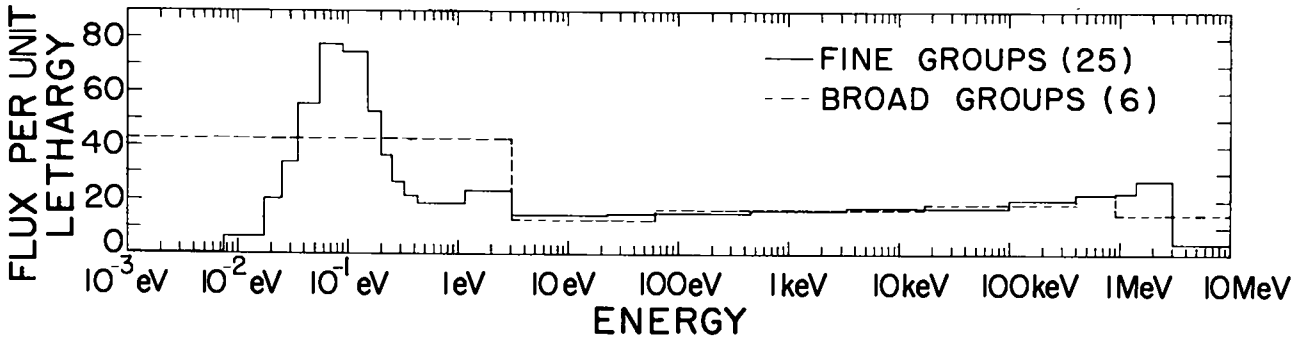

Fig. 1. Regular flux spectra for UHTREX reactor

TABLE II

BORON MICROSCOPIC CROSS SECTIONS FOR UHTREX REACTOR

25-Group Set			Collapsed 6-Group Set		
			σ^t_{boron} (barns)		
Fine Group	σ^t_{boron} (barns)	Collapsing Schemes	Broad Group	LF-Weighted	Regular-Flux Weighted
1	1.52	1	1	1.85	1.85
2	1.79		2	2.27	2.27
3	2.14		3	3.64	3.64
4	2.27	2	4	8.43	8.41
5	3.16	3	5	38.18	37.99
6	4.08		6	397.423	396.213
7	4.97	4	Collapsed 2-Group Set		
8	7.00				
9	13.00		1	11.56	11.22
10	23.50	5	2	397.423	396.213
11	36.50				
12	54.50				
13	95.8514	6			
14	149.492				
15	201.168				
16	228.955				
17	257.548				
18	292.518				
19	357.325				
20	453.072				
21	569.614				
22	694.521				
23	823.537				
24	1068.13				
25	1838.22				

1 and 2 (brackets)

It is interesting to note that the total reaction rates for boron and aluminum (the only elements investigated) using the 6-group set of LF cross sections differed by only 0.3% and 0.1%, respectively, from their initial reaction rates. The error in the ratio of these reaction rates was less than 0.3%. However, as pointed out before, if one is interested only in preserving specific reaction rates, the regular-flux method gives better values and, therefore, cross sections obtained by this method should be used for such calculations.

The new eigenvalue is calculated from

$$k_1 = \sum_{G=1}^{NBGPS} \phi_G \langle \nu\mu_f \rangle_G \ , \qquad (44)$$

where the ϕ_G are solutions of Eq. 42, using the appropriate set of collapsed cross sections as the matrix elements (either LF or regular-flux weighted). Let us define another eigenvalue

$$k_2 = \sum_{G=1}^{NBGPS} \phi^*_G \chi_G \qquad \text{(see Eq. 35).} \qquad (45)$$

With LF collapsing, $k_1 = k_2$ is always obtained, but with regular-flux collapsing, $k_1 \neq k_2$. The reasons are twofold:

1. ϕ^*_G generated with the regular-flux-weighted cross sections generally show poor agreement with the original ϕ^*_G, whereas agreement is excellent when LF-collapsed cross sections are used.

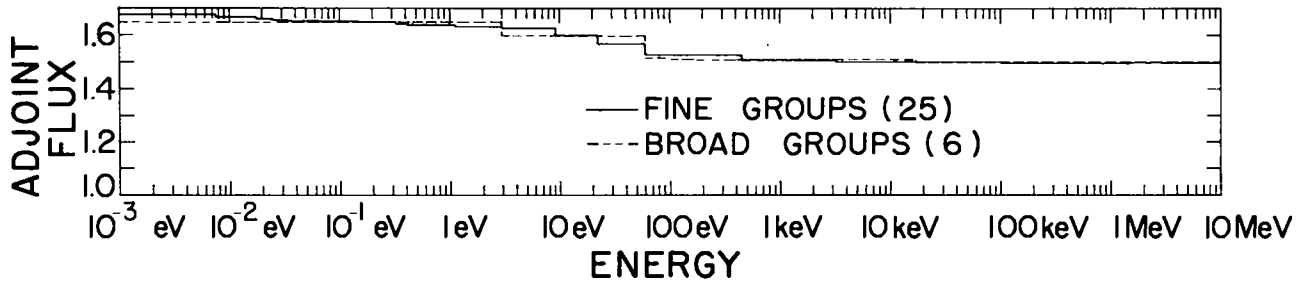

Fig. 2. Adjoint flux spectra for UHTREX reactor.

2. Even if the original ϕ_G^* are used, there is still a slight error in k_2 because the χ_g are simply accumulated in the regular-flux formation

$$\chi_G = \sum_{g \epsilon G} \chi_g \qquad (46)$$

such that the sum of the χ_G will be 1.0, whereas in the LF formulation the χ_g are weighted with ϕ_g^*.

The LF method exhibits an inherent stability to repeated collapsing. A set of one-group constants is presented in Table III. The LF formulation leads to consistent one-group constants, whether

TABLE III

ONE-GROUP CONSTANTS FOR THE UHTREX REACTOR AND THE ARGONNE FAST REACTOR

UHTREX Reactor

Group Constant	LF-Weighted		Regular-Flux-Weighted	
	25→1	25→6→1	25→1	25→6→1
k_∞	1.499	1.499	1.499	1.499
$\mu^t \times 10^{-1}$ cm^{-1}	3.508	3.508	3.486	3.486
$\mu^s \times 10^{-1}$ cm^{-1}	3.487	3.487	3.464	3.464
$\mu^a \times 10^{-3}$ cm^{-1}	2.091	2.091	2.200	2.200
$v \times 10^{5}$ cm/sec	8.871	8.871	9.277	9.276
$\ell \times 10^{-4}$ sec	5.392	5.391	5.156	5.155

Argonne Fast Reactor

Group Constant	LF-Weighted		Regular-Flux-Weighted	
	16→1	16→4→1	16→1	16→4→1
k_∞	1.425	1.425	1.425	1.425
$\mu^t \times 10^{-1}$ cm^{-1}	1.564	1.564	1.634	1.634
$\mu^s \times 10^{-1}$ cm^{-1}	1.498	1.498	1.581	1.581
$\mu^a \times 10^{-3}$ cm^{-1}	6.596	6.596	5.354	5.354
$v \times 10^{8}$ cm/sec	4.878	4.878	4.222	4.222
$\ell \times 10^{-7}$ sec	3.108	3.108	3.591	3.591

the collapsing scheme is 25→1 or 25→6→1. The regular-flux method also leads to fairly consistent results, but the agreement is not as good as with the LF method. Collapsing schemes 25→2 and 25→6→2 showed similar results. Different values were predicted for neutron velocity and lifetime by the two weighting methods. The broad-group fluxes from Eqs. 15 and 42 for the collapsing scheme shown in Table II are given in the first part of Table IV.

TABLE IV

BROAD-GROUP FLUX SPECTRA FOR THE UHTREX REACTOR

Regular Fluxes

Broad Group	Eq. 15	Eq. 42 with LF-Weighted Cross Sections	Eq. 42 with Regular-Flux-Weighted Cross Sections
1	36.08	36.08	36.08
2	18.13	18.13	18.13
3	58.50	58.50	58.50
4	91.97	91.98	91.97
5	44.93	44.93	44.94
6	204.89	204.89	204.91

Adjoint Fluxes

Broad Group	Eq. 16	Eq. 43 with LF-Weighted Cross Sections	Eq. 43 with Regular-Flux-Weighted Cross Sections
1	1.499	1.499	1.499
2	1.499	1.499	1.499
3	1.500	1.500	1.499
4	1.511	1.511	1.503
5	1.595	1.595	1.564
6	1.647	1.647	1.630

In Table IV, the agreement of columns 2 and 3 is only slightly better than that observed between columns 2 and 4. It is interesting to note, however, that column 4 shows its poorest agreement in group 6, which is the severest collapsing test, since it contains the most fine groups (see Table II). In contrast, the ϕ_G calculated from LF-weighted cross sections agreed with column 2 consistently for all cases investigated, regardless of the collapsing scheme chosen. The second part of Table IV presents the results for the adjoint flux. Here the agreement of the first two sets of adjoint fluxes is notably better than that of the first and third sets. These results are typical of all collapsed sets of cross sections which were investigated. In all cases, the LF cross-section sets yielded more consistent values for the regular and adjoint fluxes of the reactor.

6.3 16-Group Set of Argonne Fast Reactor Cross Sections[7]

The nuclide mix from the central core region of the Argonne Fast Reactor[7] was used for the following calculations. The 16-group flux spectrum (per unit lethargy) is plotted in Fig. 3, except for the low-energy groups where the flux was negligible. Superimposed on this set of fluxes is a set of

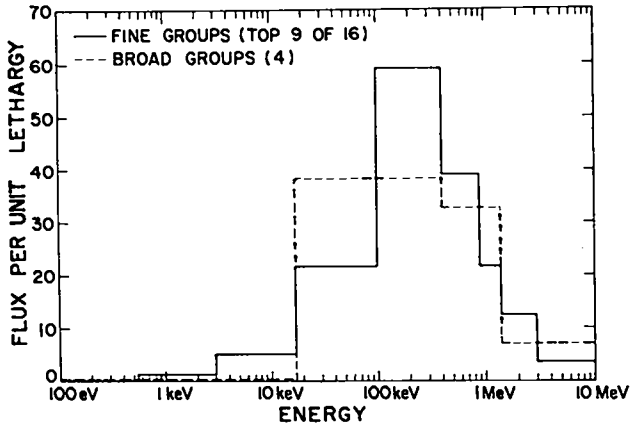

Fig. 3. Regular flux spectrum for the Argonne Fast Reactor.

TABLE V

MICROSCOPIC CROSS SECTIONS FOR ^{239}Pu ARGONNE FAST REACTOR

16-Group Set			Collapsed 4-Group Set		
				σ^t_{Pu} (barns)	
Fine Group	σ^t_{Pu} (barns)	Collapsing Schemes	Broad Group	LF-Weighted	Regular-Flux-Weighted
1	4.25	1	1	4.42	4.42
2	4.5		2	5.48	5.49
3	4.8	2 → 1	3	9.66	9.93
4	5.69999		4	14.73	14.60
5	8.39999	3			
6	13.1999		Collapsed 2-Group Set		
7	13.4999	4 → 2	1	8.03	8.45
8	16.6999		2	14.73	14.60
9	34.2999				
10	35.0999				
11	65.1999				
12	26.6999				
13	33.0				
14	171.599				
15	1300.0				
16	990.0				

broad-group fluxes (4 groups). The corresponding adjoint fluxes are plotted in Fig. 4. The total macroscopic cross sections are shown in Fig. 5.

Microscopic cross sections for ^{239}Pu are given in Table V. The cross sections of energy groups 9 through 16 were weighted very lightly, because the flux in those groups was practically negligible. Since the adjoint flux in the Argonne Fast Reactor is more irregular than that in the UHTREX reactor, the LF-weighted cross sections and the regular-flux-weighted cross sections in the Argonne reactor will not agree as closely as they did in the UHTREX calculations. The one-group constants for the Argonne Fast Reactor are given in Table III. The regular and adjoint flux spectra generated by both sets of 4-group cross sections are given in Table VI.

7. CONCLUSIONS

The LF method is a complete and accurate method of collapsing cross sections. For the infinite-medium problems which were discussed in the report, the eigenvalue, broad-group regular fluxes, and broad-group adjoint fluxes predicted by the fine-group calculations are preserved when computed with the LF-weighted cross sections. The agreement with the fine-group calculations was as good as, or slightly better than, the agreement afforded by the regular-flux-weighted cross sections, but the difference between the two methods was not substantial for infinite-medium problems. The regular-flux-weighted cross sections are preferable for the preservation of reaction rates.

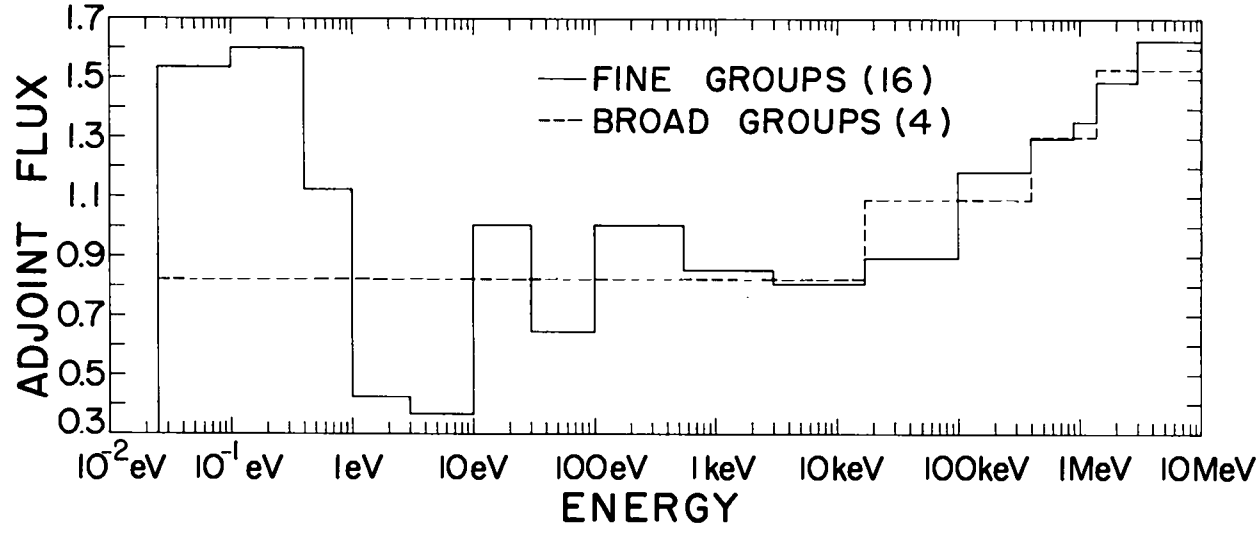

Fig. 4. Adjoint flux spectrum for the Argonne Fast Reactor.

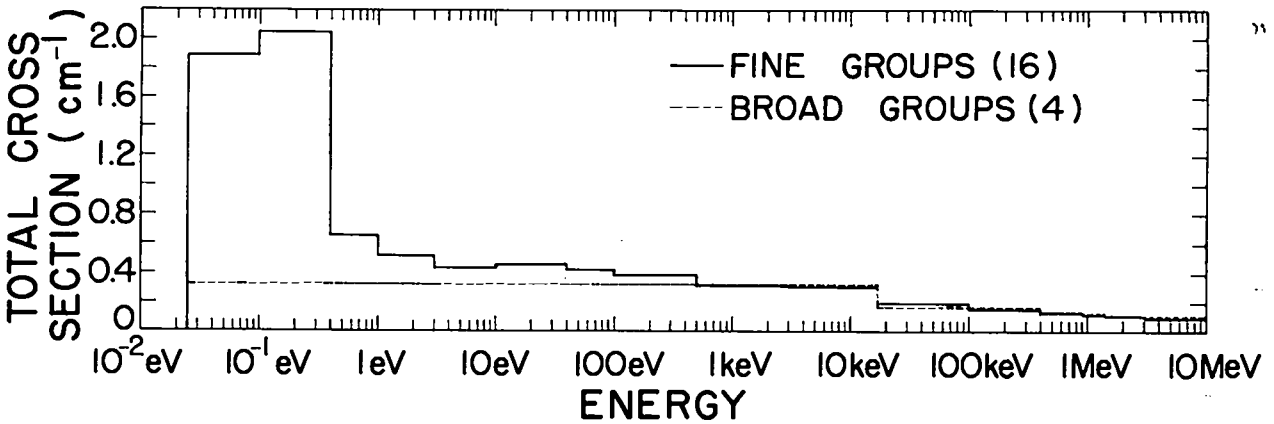

Fig. 5. Total macroscopic cross sections for the Argonne Fast Reactor.

TABLE VI

BROAD-GROUP FLUX SPECTRA
ARGONNE FAST REACTOR

Regular Fluxes

Broad Group	Eq. 15	Eq. 42 with LF-Weighted Cross Sections	Eq. 42 with Regular-Flux-Weighted Cross Sections
1	13.82	13.82	13.82
2	41.27	41.27	41.27
3	120.5	120.5	120.5
4	11.20	11.20	11.19

Adjoint Fluxes

Broad Group	Eq. 16	Eq. 43 with LF-Weighted Cross Sections	Eq. 43 with Regular-Flux-Weighted Cross Sections
1	1.534	1.534	1.540
2	1.309	1.309	1.323
3	1.092	1.092	1.156
4	0.822	0.822	0.808

The space-dependent problem presents a more rigorous and more important test of the LF collapsing technique. Investigation in this area is now under way. For most applications, few-group cross sections can be constructed by the regular-flux weighting method, but for reactivity coefficient calculations, flux-weighted cross sections are often inadequate. The LF method of collapsing may improve the accuracy of these calculations.

REFERENCES

1. D. S. Selengut, "Variational Analysis of Multi-Dimensional Systems," Nuclear Physics Research Quarterly Report HW-59126, 89, Hanford Atomic Products Operation, General Electric (January 20, 1959).

2. W. W. Little and R. W. Hardie, "Methods for Collapsing Fast Reactor Neutron Cross Sections," Nucl. Sci. Eng. 29, 402 (1967).

3. "UHTREX Facility Description and Safety Analysis Report," LA-3556 (Revised), Los Alamos Scientific Laboratory (1967).

4. "Los Alamos Group Averaged Cross Sections," L. D. Connolly, ed., LAMS-2941, Los Alamos Scientific Laboratory (1963).

5. G. E. Hansen and W. H. Roach, "Six and Sixteen Group Cross Sections for Fast and Intermediate Critical Assemblies," LAMS-2543, Los Alamos Scientific Laboratory (1961).

6. J. C. Vigil, private communication (1966).

7. "Argonne 1000 MW(e) Metal Fueled Fast Breeder Reactor," ANL-7001, Argonne National Laboratory (1966).

APPENDIX A - CHILE

For each collapsing scheme, two complete sets of broad-group macroscopic cross sections and χ factors are punched. The broad-group regular and adjoint fluxes from Eqs. 15 and 16 are also punched out. One set of broad-group cross sections is collapsed by the regular-flux method, and the other by the LF method. These cross sections appear on the printout along with the results of a one-group collapse, which is always calculated regardless of the specific collapsing scheme requested. It should be noted that the adjoint-weighted χ factors do not, in general, sum to 1.0. This fact is not surprising, since this method imposes no restriction on the broad-group χ's. Physically, the broad-group χ's represent a perturbed fractional distribution of fission neutrons. This leads to an interesting result in the one-group case. Since the multiplication factor, k, is the total number of fission neutrons divided by the total number of neutrons absorbed, then

$$k = \frac{\chi\langle\nu\mu_f\rangle}{\mu_a} .$$

Normally, χ would be defined as 1 when setting up a one-group problem, and k reduces to:

$$k = \frac{\langle\nu\mu_f\rangle}{\mu_a} .$$

However, when LF weighting is used to collapse multigroup cross sections, χ generally will not equal 1.

CHILE can easily be extended to compute microscopic collapsed cross sections by storing the fine-group cross sections for each element on a scratch tape and recalling them, element by element, after the multigroup equations have been solved. This has been done for the 59-group set of thermal cross sections.

INPUT SPECIFICATIONS FOR CHILE

Card	Format	Entry	Description
1	12A6	A(I),I=1,12	Title card for problem
2	12I6	NFGPS	Number of fine groups
		NBGPS	Number of broad groups
		NELEMT	Number of nuclides in the mixture
3	12I6	NK(N)	Highest fine group included in broad group N
4	12I6	NG(N)	Lowest fine group included in broad group N
5	6E12.5	E(I),I=1,LFGPS where LFGPS=NFGPS+1	Fine-group upper energy boundary (eV)(except for the last entry, which is the lower boundary of the lowest energy group)
6	6E12.5	VEL(I),I=1,NFGPS	Fine-group velocities (cm/shake)
7	6E12.5	S(I),I=1,NFGPS	Fine-group sources (fission spectrum)
Repeat cards 8-11 for each nuclide.			
8	12A6	AID(I),I=1,12	ID card for nuclide
9	6E12.5	ADEN	Atom density (10^{-24} atoms/cc)
Cards 10 and 11 are for 16 fine groups; they must be repeated 16 times.			
10	6E12.5	USLES1	Not used
		XF(I)	Fission cross section for group I
		XS(I)	Scattering cross section for group I
		XA(I)	Absorption cross section for group I
		XFN(I)	$\nu\sigma_f$
		XTOT(I)	Total cross section
11	6E12.5	GTRANS(I,I)	σ^s(I→I)
		GTRANS(I-1,I)	σ^s(I-1→I)
		GTRANS(I-2,I)	σ^s(I-2→I)
		GTRANS(I-3,I)	σ^s(I-3→I)
		GTRANS(I-4,I)	σ^s(I-4→I)
		GTRANS(I-5,I) I=1,NFGPS	σ^s(I-5→I)
For 25 groups replace cards 10 and 11 by card 10^A.			
10^A	6E12.5	XA(I)	σ^a(I)
		XFN(I)	$\nu\sigma^f$(I)
		XTOT(I)	σ^t(I)
		USLES1	See card 10
		GTRANS(I+4,I)	σ^s(I+4→I)
		GTRANS(I+3,I)	σ^s(I+3→I)
		GTRANS(I+2,I)	σ^s(I+2→I)
		GTRANS(I+1,I)	σ^s(I+1→I)
		GTRANS(I,I)	See card 11
		GTRANS(I-1,I)	See card 11
		GTRANS(I-2,I)	See card 11
		GTRANS(I-3,I)	See card 11
		GTRANS(I-4,I) I=1,NFGPS	See card 11

APPENDIX B

TAOS

A second code, TAOS, solves the multigroup Eqs. 2 and 4 for a reduced number of groups using the collapsed cross sections as input data. Both LF-weighted cross sections and regular-flux-weighted cross sections are tested by this code; TAOS contains an optional routine for collapsing to an even smaller number of groups. Primarily, however, TAOS makes it possible to use the collapsed cross sections for generating broad-group regular and adjoint fluxes. The output of TAOS displays these fluxes next to the fluxes which were defined earlier in terms of the fine-group regular and adjoint fluxes (see Eqs. 15 and 16). This program also computes the new eigenvalue from Eq. 44 (written for a reduced number of groups) and compares it with the initial eigenvalue.

INPUT SPECIFICATIONS FOR TAOS

Fine-group input for TAOS is the collapsed output from CHILE.

Card	Format	Entry	Description
1	12A6	A(I),I=1,12	Title card for problem
2	12I6	NFGPS	Number of input groups (broad groups from initial collapse)
		NBGPS	Number of broad groups (for multiple collapsing)
		NELEMT	Number of nuclides in the mixture
3	12I6	NK(N),N=1,NBGPS	Highest fine group included in broad group N
4	12I6	NG(N),N=1,NBGPS	Lowest fine group in broad group N
5	6E12.5	OLDEIG	Original eigenfunction of the reactor (calculated in CHILE)
6	6E12.5	E(I),I=1,LFGPS	Fine-group upper energy boundary (eV) (except for the last entry, which is the lower boundary of the lowest energy group).
7	6E12.5	VEL(I),I=1,NFGPS	Fine-group velocity
8	6E12.5	S(I),I=1,NFGPS	Sources
Repeat cards 9 and 10 for each nuclide.			
9	12A6	AID(I),I=1,NFGPS	ID card for nuclide
10	6E12.5	ADEN	Atom density collapsed (10^{-24} atoms/cc)
11	6E12.5	SIGA(I),I=1,NFGPS	Macroscopic absorption cross sections from CHILE
12	6E12.5	FISNU(I),I=1,NFGPS	$\langle \nu\mu^f \rangle_G$ from CHILE
13	6E12.5	SIGTOT(I),I=1,NFGPS	μ_G^t from CHILE
14	6E12.5	((EKVR(I,J),J=1, NFGPS),I=1,NFGPS)	$\mu^s(G \rightarrow G')$ macroscopic transfer matrix from CHILE
15	6E12.5	OLDPHI(I),I=1,NFGPS	Defined regular fluxes from CHILE
16	6E12.5	OLDPHIA(I),I=1,NFGPS	Defined adjoint fluxes from CHILE

APPENDIX C

INPUT SPECIFICATIONS FOR THMOD

Card	Format	Entry	Description
1	12A6	A(I),I=1,12	Title card for problem
2	12I6	NFGPS	Number of fine groups
		NBGPS	Number of broad groups
		NABS	Number of absorbers
		NKER	Number of scatterers
3	12I6	NK(N),N=1,NBGPS	Highest fine group included in broad group N
4	6E12.5	EPSI	Convergence criterion on calculated flux (not used)
		DBS	DB^2 leakage allowance factor
5	6E12.5	E(I)	Fine-group upper energy boundaries (eV)
Repeat cards 6-10 for each absorber			
6	12A6	AID(I),I=1,12	ID card for absorber
7	6E12.5	ADEN	Atom density (10^{-24} atoms/cc)
		ANU	ν(ANU = 0 for nonfissile nuclide)
8	6E12.5	XA(I),I=1,NFGPS	Absorption cross sections by fine groups (barns)
9	6E12.5	XS(I),I=1,NFGPS	Scattering cross sections by fine groups (barns)
10	6E12.5	XF(I),I=1,NFGPS	Fission cross sections by fine groups (barns) (omit card 10 if ANU=0)
Repeat cards 11-15 for each scatterer			
11	12A6	AID(I),I=1,12	ID card for scatterer
12	6E12.5	T	Temperature of scatterer (°K)
		FSX	Free atom scattering cross section (barns)
		ADEN	See card 7
13	6E12.5	XA(I),I=1,NFGPS	See card 8
14	6E12.5	XS(I),I=1,NFGPS	See card 9
15	6E12.5	VEC(M),M=1,5 I≥J,J=1,NFGPS	Half kernel from SUMMIT
16	6E12.5	S(I),I=1,NFGPS	Fine-group sources